Adhesion of yield stress fluids

Quentin Barral, Guillaume Ovarlez, Xavier Chateau, Jalila Boujlel, Brooks Rabideau, Philippe Coussot

Adhesion of yield stress fluids

Q. Barral, G. Ovarlez, X. Chateau, J. Boujlel, B. Rabideau, P. Coussot

Université Paris-Est, Institut Navier, LMSGC, Champs sur Marne, France

Abstract: The different regimes of flow when separating two solid rough surfaces in contact via a layer of a simple yield stress fluid are identified. Generic scalings for the adhesion energy and for the geometrical characteristics of the final deposits (after separation) as a function of the initial aspect ratio of the sample are found. We show that there is a strong pinning effect which might be at the origin of an adhesion energy significantly larger (by a factor about 2) than that estimated from the lubrication theory. We also observe that the conditions of development of viscous fingering are not at all predicted by the conventional Saffman-Taylor instability theory taking into account the specific non-Newtonian character of the fluid. This again suggests that for pastes the pinning effect plays a significant stabilizing role.

1. Introduction

Many industrial processes involve the adhesion of materials which are not adhesives in the basic sense, i.e. they are not viscoelastic solids only. These include certain glues before solidification, mortars or rendering, plasters, fouling deposits in the food and mineral industries, mud deposits on tools in drilling or tunneling process, cosmetic creams or foams on skin, etc. All of these materials belong to the class of jammed systems [1], or *pastes*, made of a high concentration of mesoscopic elements jammed in a volume of liquid. These materials have been the object of intense research in recent years [2-6] and there is now a consistent knowledge of their bulk properties. However the knowledge of their interfacial properties is still extremely poor, in contrast with that of simple solids and liquids [7]. One basic question, which has been poorly addressed until now, although of fundamental practical importance in the above examples, concerns the energy of adhesion required to separate two solid surfaces in contact via a layer of pasty material.

Pastes include a wide range of materials such as colloids, gels, foams, emulsions, suspensions, and various other more complex systems such as sewage sludge, foodstuffs, mortars, etc. Typically these systems contain a structure of elements in interaction which is jammed and immersed in an interstitial liquid phase. The jammed character finds its origin in that the elements are unable to get out of the structure with thermal agitation only. An external force is

needed to push them from their local cage and break the structure. Typically such materials exhibit a solid viscoelastic behavior below a critical deformation, and a viscoplastic behaviour beyond this critical deformation. In addition they may be thixotropic, i.e. their resistance to deformation or flow depends on the flow history. This thixotropic character is more or less marked depending on materials. Recently it was shown that the solid-liquid transition may lead to very different trends depending on the material structure [8-9] but that it was finally suggested [10] that these fluids may be classed into two main categories according to the predominant type of interaction within the structure: mainly repulsive systems (moderately concentrated foams, microgels, emulsions) behave as simple yield stress fluids with a continuous transition from the solid to the liquid regime; mainly attractive systems (various colloidal suspension types with appropriate interactions), exhibit an abrupt transition from the solid to the liquid regime: no steady flow can occur below a critical shear rate, so that when a lower apparent shear rate is imposed the flow is heterogeneous (shear-banding). In the present work we focus on the adhesion behaviour of systems of the first group, i.e. simple yield stress fluids with a smooth solid-liquid transition and a negligible thixotropic character.

In an adhesion test two solids separated by a layer of material are moved away from each other. Such a process implies the creation of new interfaces, but in general the required energy is much higher than typical surface energies. This means that the process involves the deformation or flow of the material between the two moving solid surfaces. A usual procedure for measuring the adhesive properties of materials is the probe tack test in which a solid surface is brought into contact with an adhesive layer, and after a certain waiting time, pulled away at a fixed speed. The force vs (separating) distance in time is then recorded, from which we can deduce the total adhesion energy. For simple liquids the induced inwards radial flow (due to its incompressibility the liquid gathers towards the center as its thickness increases) may be described in details within the frame of the lubrication theory as long as the gap between the solid surfaces is much smaller than the size of the surface of contact between the liquid and the solid [11]. This provides a theoretical expression for the adhesion energy as a function of the material viscosity. For solids this process may induce among others breakage, cavitation, filament formation or instability [12]. Recent studies have started to clarify the role of elastic or viscous instabilities in the adhesion process for viscoelastic materials [13-17].

Adhesion of yield stress fluids might lead to specific effects since they could borrow their adhesion behaviour both from solids and from liquids. For such materials this process was mainly studied via the observed fingering patterns [18-20]. The only study in this field [20]

which also dealt with the adhesion energy showed that under some conditions it finds its origin in the viscous dissipation. Besides, the authors found that in their specific range of observation the order of magnitude of the experimental fingering wavelength was well predicted by the Saffman-Taylor instability theory, but there remained some unexplained discrepancy between theory and data concerning the variations of this wavelength.

Here we provide a systematic analysis of the different regimes of paste adhesion from a series of experiments with model materials for different yield stresses, volumes and layer thicknesses. Generic scalings for the adhesion energy and for the geometrical characteristics of the final deposits (after separation) are identified. For such materials the adhesion process appears to be strongly affected by a pinning effect, i.e. as long as wall slip is avoided there is no dewetting, the line of contact remains fixed. In the stable regimes this effect significantly increases the adhesion energy as compared to the theoretical energy under the lubrication assumption. Moreover it might tend to stabilize the interface precluding viscous fingering in the range expected for the development of the Saffman-Taylor instability.

2. Materials and procedures

2.1 Materials

A typical model, a simple yield stress fluid was used, solutions of Carbopol (*Carbopol U10*) in water, whose structure is essentially that of a “glass comprised of individual elastic micro-sponges” [21]. Inspite of this statement it is usual to name them “Carbopol gels”. A 0.4% (volume fraction) Carbopol gel (Gel 1) and a 1.5% solution (Gel 2) were used (see preparation procedure in [22]). Here we only present quantitative data obtained with these materials but we also carried out tests with another material of similar rheological behaviour, a concentrated emulsion (see material characteristics in [23]), which yielded similar qualitative results and tends to confirm the generality of our findings for simple yield stress fluids. All the lengthscales involved in our experiments are much larger than the lengthscale of the material elements (which is supposed to be comprised in the range 1-10 microns), so that they can be considered as continuous materials in this context.

2.2 Solid surfaces

It has for long been observed that pasty materials, and in particular Carbopol gels [24] may slip along solid wall [25]. In that case there is an apparent discontinuity in the velocity profile at the approach of the wall, and the mean fluid velocity is larger than expected from a homogeneous flow of the bulk under the same external stress conditions. It is widely admitted that for such materials wall slip is due to a slight depletion of elements at the approach of the wall, leading to a thin layer of less viscous material flowing at a larger shear rate than the bulk for the same stress. Thus the apparent macroscopic behaviour is affected by the specificities of the solid surface characteristics and the local structure of the paste.

Here we intend to focus on phenomena strictly involving generic bulk and surface properties. In that aim we used solid surfaces made with waterproof sandpaper attached to solid surfaces. The average particle diameter of this sandpaper was 82 μm, leading to an effective roughness of a few tenths of microns, a dimension still much larger than the typical element size of Carbopol gels. Since the volume loss in the roughness could be significant in some cases, a generous amount of extra sample was applied to the surface of the sandpaper before each test and the excess removed by scraping the surface with a palette knife. This also ensured reproducible wetting conditions of the fluid onto the solid surface. Between two successive tests, both plates were removed and cleaned.

Under these conditions the contact of the bulk with the solid surface is set up via the contact of the bulk with a set of fluid inclusions which, due to their yielding character, are in general more or less blocked in the holes of the rough surface. As a consequence the volume of paste able to flow may be considered as mainly in contact with a thin layer of fixed paste volume. In such a situation only the bulk properties of the paste are involved in the solid-paste interaction. The distance between the solid plate was measured from the contact between the rough surfaces before setting up the sample, which corresponds to the contact between the virtual planar surfaces covering these rough surfaces. Note that for some tests the initial thickness of the sample layer between the plates was in the range [15-50] microns. This likely increased the uncertainty on data but did not seem to affect the process characteristics: we did not observe any specific aspect of the sample at the end of the test or of the force vs distance curve trends.

2.3 Rheometry

The preparation and rheometrical characterization of these materials is described in [22]. Typically they behave as viscoelastic solids below a yield stress (τ_c) associated with a critical deformation. This is the solid regime, illustrated by the fact that for creep tests at a stress level below τ_c the material initially deforms then the deformation tends to saturate. In contrast, for stresses larger than τ_c, after some time the deformation increases at a constant rate corresponding to a steady state flow: this is the liquid regime. As for other similar yield stress fluids the flow curve (shear stress (τ) vs shear rate ($\dot{\gamma}$) curve in steady state simple shear) is very well represented by a Herschel-Bulkley model (see Fig.1):

$$\tau > \tau_c \Rightarrow \tau = \tau_c + k\dot{\gamma}^n \qquad (1)$$

in which k and n are material parameters. The usual 3D form of the constitutive equation in the liquid regime, extrapolated from equation (1), is a stress tensor equal to the sum of a term proportional to the yield stress and a term depending on the flow rate [25].

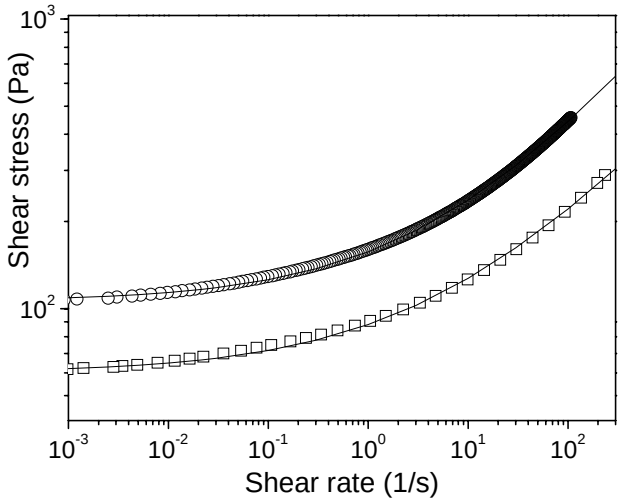

Figure 1: Flow curves of the two Carbopol gels used in this study (squares: 0.4%; circles: 1.5%). The continuous lines are the Herschel-Bulkley model fitted to each set of data with the following parameters: $\tau_c = 60\text{Pa}, k = 28\text{Pa.s}^n, n = 0.38$ (0.4%), $\tau_c = 106\text{Pa}, k = 51\text{Pa.s}^n, n = 0.41$ (1.5%).

2.4 Squeeze and traction tests

For the adhesion tests a dual-column testing system (*Instron* model 3365) with a position resolution of 0.118 μm was used. The column was equipped with either a 10 or 500 N static

load cell which were able to measure the force to within a relative value of $\pm 10^{-6}$ of the maximum value. The plate surfaces were prepared as described in Section 2.2. A given volume of material was then collected with a syringe, put at the center of the bottom plate, and the upper plate was decreased at a fixed (initial) height (h_0), thus squeezing the material. The adhesion test then consisted of lifting the upper plate at a constant velocity ($0.01\,$mm/s, unless noted otherwise) while monitoring the force (F) applied to the upper plate. For some critical distance h_c the force rapidly drops to zero (see Fig.2), an effect associated with the separation of the sample into two parts.

3. Theoretical considerations

3.1 Adhesion energy

In order to quantify paste adhesion a parameter which globally quantifies the level of the force vs distance curve is the energy needed for complete separation: $W = \int_{h_0}^{h_c} F dh$. Note that due to the low induced velocities the inertia is negligible. As the upper plate is moved upwards different types of phenomena occur, which are at the origin of different sources of energy:

- Flow of the material leading to viscous (or plastic) dissipation: W_v;
- Surface energy change due to the change of the areas of the interfaces: W_s;
- Gravity work due to the upward motion of the sample: W_g.

In addition, with yield stress fluids energy may be stored in the material in the form of elasticity in the solid regime, in particular during the squeeze flow setting up the sample in its initial state. The corresponding energy per unit volume is of the order of $G\varepsilon^2/2$, in which ε is the critical deformation at the solid-liquid transition (typically of the order of 20%) and G the shear modulus (of the order of τ_c/ε). In our case this gives (for Gel 1) a maximum elastic energy possibly stored in the material of the order of $6\,\mathrm{J.m^3}$ while the energy measured is larger by a factor ranging from 10 to 1000. As a consequence we will neglect the possible elastic energy stored in the material.

The work of gravity corresponds to the energy needed to move upwards a part of the sample. Since the shapes of the paste deposits on each plate are similar (see below) after the separation associated with the distance h_c, each element at a distance $h_c - d$ above the lower

plate surface has its counterpart displaced at a distance d. Thus all occurs as if half the material was displaced vertically at a distance h_c from the initial distance h_0 while the rest of material remained fixed. The gravity work is thus:

$$W_g = \frac{1}{2}\rho g \Omega \left(h_c - h_0\right) \qquad (2)$$

This energy is not negligible for low initial aspect ratio. For our data analysis we have withdrawn the corresponding term from the total energy measured. This makes it possible to focus on the *adhesion energy* that we define as $W_{\text{adhesion}} = W_S + W_V$.

Our tests at different rates of separation ($\dot{h} = V$) show that W_{adhesion} tends to a plateau for low velocities (see inset of Fig.4). This means that there is a minimum adhesion energy (W_P) required for separation, which is independent of the separation rate. This implies that, if viscous dissipation is significant only the flow rate-independent term in the stress tensor plays a role. All the tests presented in this paper were carried out at a velocity (0.01mm/s) for which $W_{\text{adhesion}} \approx W_P$.

3.2 Lubrication theory

The so-called squeeze flow of yield stress fluids between two approaching solid plates has been the object of much work (see for example [22, 26-27]). The classical theoretical treatment [28] considers the flow of a yield stress fluid in its liquid regime within the frame of the so-called lubrication assumption. It is assumed that, in the absence of wall slip and when the distance h is much smaller than the radius R of the layer, most of the material undergoes a flow which is instantaneously locally similar to a radial simple shear flow. From the momentum equation we find the relation between the shear stress and the pressure distribution $p(r)$:

$$\tau = \tau_{rz}(r,z) = \left(\frac{\partial p}{\partial r}\right) z \qquad (3)$$

in which z is the height above the midplane of the sample. At each distance r from the central vertical axis the maximum stress amplitude is reached along the plates ($z = \pm h/2$) and a flow of the sample in the liquid regime implies that the yield stress is at least overcome, i.e. the material is in its liquid regime, everywhere along the walls. We focus on the case of slow

flows for which the shear-rate dependent term in the constitutive equation is negligible with regards to the yield stress term, so that in the liquid regime $\tau \approx \tau_c$. In that case the integration of (3) between R and r assuming no surface tension effect and negligible atmospheric pressure provides the pressure distribution:

$$p(r) = \frac{2\tau_c}{h}(r - R) \tag{4}$$

The net normal force exerted onto the plate in that case is found by integrating the pressure expression (4) over the surface of contact in this limiting case:

$$F = -\int_0^R 2\pi r p(r) dr = \frac{2\pi\tau_c R^3}{3h} \tag{5}$$

Note that this expression was found to be in good agreement with experimental data for tests done under well controlled conditions [22]. The corresponding adhesion energy follows:

$$W_P = 4\tau_c S_0^{1.5} / 9\sqrt{\pi} \tag{6}$$

in which $S_0 = \pi R_0^2$ is the initial surface of contact of the paste with the solid surfaces. Actually the expression (6) strictly derives from (5) if the sample keeps a cylindrical shape and if the lubrication assumption remains valid until the material separation into two parts. These hypotheses are likely wrong in most cases since the separation appears to occur for h of the order of R. In that case, i.e. outside the range of validity of the lubrication assumption and up to $h \approx R$, the flow characteristics can hardly be described analytically but it is likely that the value obtained from the normal force expression (5) is larger than the effective value since the fluid is less constrained by the walls. This suggests that in our context (6) should be generally considered as an upper boundary of the effective viscous adhesion energy term. Moreover the expression (6) tends to the exact value when the initial aspect ratio tends to very large values since then the lubrication regime prevails during most of the flow.

3.3 Surface interactions

During an adhesion test the paste moves along the solid surface and separates into two parts, which implies that the surface energies associated with changes of the interface areas may be significant. Actually the knowledge concerning the interfacial tension of pastes with solid or gas is extremely poor. It has been assumed [25, 29] that the surface tension of pastes (i.e. the

interfacial tension of paste with air) is equal to that of the interstitial liquid, since the latter coats all the elements of the structure and thus the paste-air interface should in fact be an interstitial liquid-air interface. Only recently a unique study directly attempted to measure the surface tension of a gel from periodical laser irradiation of the surface, with results tending to confirm the above assumption [30]. According to this conclusion, since water is the interstitial liquid of our gels the surface tension would be equal to the typical value for water at 20°C, i.e. $\gamma = 0.072$ Pa.m but we will have the opportunity to check this assumption from our data (see Section 4.2).

The question of the paste-solid interaction is potentially more complex as the interstitial liquid and the paste elements may interact separately with the solid surface. Here we avoid this problem by using rough surfaces filled with a thin layer of gel. Thus the paste-solid contact is in fact a paste-paste contact, and as the paste front withdraws along the solid surface during an adhesion test the roughness holes remain filled with some paste. Thus there is no real dewetting (in the usual meaning) of the paste from the solid surface. This in particular implies that one cannot consider the contact angle as reflecting an intrinsic property of the material. On the contrary, as will be seen later the shapes of the interfaces at the line of contact entirely depend on the flow history.

In this context the surface energy increase as a result of plate separation is then simply equal to $\gamma \Delta S$, in which ΔS is the increase of air-paste area. This area increase depends on the exact shape of the deposit on each plate after separation. Two limiting cases may usefully be considered. If at the end of the test the paste forms approximately a uniform layer (typically when $R_0/h_0 >> 1$) we have $\Delta S \approx 2\pi R_0^2$. If on the contrary the final shape on each plate is a cone of equal radius and height (which typically occurs when $R_0/h_0 \approx 1$): $\Delta S \approx 1.5\pi R_0^2$. The general case is intermediate between these two cases: the air-paste interface includes planar and conical regions, so that we can expect that ΔS will vary around $2\pi R_0^2$, and finally we have $W_s \approx 2\pi\gamma R_0^2$.

3.4 Saffman-Taylor instability

A phenomenon often observed when stretching a paste between two plates is the formation of fingers at the periphery of the samples evolving in tree-like structures after complete separation [18-20, 31]). Such structures are commonly observed in various practical situations

when one separates two solid surfaces initially in contact via a thin layer of mud, glue, paint, puree, etc. This phenomenon occurs with simpler liquids, for example Newtonian, but in that case only at a sufficiently large rate of separation of the solid surfaces.

These different characteristics are typical of the Saffman-Taylor instability [32] for simple [33] or yield stress fluids [34] which occurs when a viscous fluid is pushed by a less viscous one, for example a liquid pushed by a gas, and results from a competition between surface tension and viscous effects. When viscous effects are sufficiently large compared to interfacial effects the flow along parallel channels separated by regions flowing at a very small rate is more favourable as it dissipates less energy. The origin of this phenomenon may be understood for radial flows from the following heuristic arguments. Let us assume that the interface, initially circular in a horizontal plane (r,θ), undergoes a perturbation in the form of a sinusoid of wavelength k (such that $k = 2\pi/\lambda > 1/R$) and small amplitude ε. From (4) we can estimate the additional viscous pressure drop induced by an additional flow over the distance ε: $2\tau_w\varepsilon/h$, in which τ_w is the wall shear stress. The corresponding pressure difference due to surface tension effects as a result of this additional curvature of the interface in (r,θ) may be estimated as $\gamma k^2\varepsilon$. The instability appears when the former pressure drop is larger than the latter (i.e. when $2\tau_w/h > \gamma k^2$). Indeed the net pressure drop then tends to push farther the fluid which amplifies the perturbation. This approach effectively predicts that the instability disappears for sufficiently slow flows when τ_w, which is proportional to the velocity for a Newtonian fluid, is sufficiently small. During an adhesion test the distance between the solid surfaces changes in time. However, as long as the gap size remains much smaller than the typical length of the surface of contact between the fluid and the solid, the separation mainly induces a flow of the fluid towards the central axis, the stability of which should be described with the usual Saffman-Taylor theory for constant gap.

For Newtonian fluids the instability is apparent only when the front width is larger than the wavelength of maximum growth (λ_m), which decreases when the velocity or the viscosity increases [33], so that the instability appears only when the velocity is sufficiently large. Complementary developments have been proposed for different types of non-Newtonian fluids [35-37], leading to similar qualitative characteristics. A strong difference with yield stress fluids is that, as the fluid velocity tends to zero the wall stress tends to a finite value, i.e. the yield stress: $\tau_w \to \tau_c$. This implies that λ_m is larger than a finite value for very slow flows. The existing linear stability theory for yield stress fluids [34] provides

$\lambda_m = 2\sqrt{3}\pi R\left(1+2\tau_c R^2/\gamma h\right)^{-1/2}$ and the criterion for the apparent onset of instability for radial flows:

$$\tau_c > \frac{\gamma h}{R^2} \tag{7}$$

A reasonable agreement of this theory with experiments was found concerning the wavelength of maximum growth [20, 38] in some limited range of parameters but no serious attempt to compare the predictions for the conditions of occurrence with the observations was carried out so far.

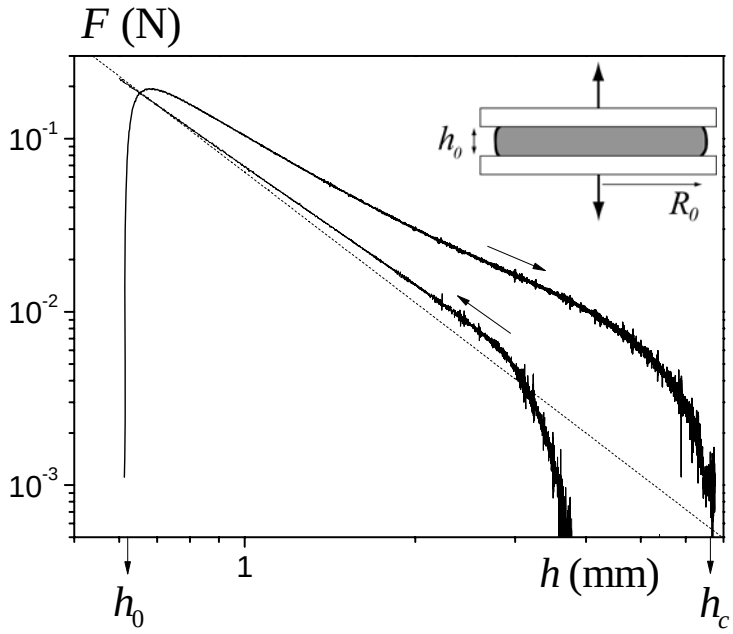

Figure 2: Squeeze test (lower curve) immediately followed by a separation test (upper curve) with the same sample (Gel 1, $\Omega = 0.2\text{ml}$): force amplitude vs distance. The dotted line corresponds to equation (5) expressed as a function of h only: $F = 2\Omega^{3/2}\tau_c h^{-5/2}/3\sqrt{\pi}$.

4. Results

4.1 Force vs distance

Squeeze flows

Let us first look at the curve of force vs separation distance (h). During the preliminary squeezing phase the force increases as the distance decreases (see Fig.2) inducing material deformation. During this phase the material likely first undergoes some elastic loading in its solid regime then, beyond a critical deformation, a transition to its liquid regime. The exact point at which the transition between the solid and the liquid regime occurs remains unclear, but it is certain that it occurs beyond a sufficiently large overall deformation. It was shown that the lubrication model (see Section 3.2) is able to predict rather well the distance vs time curves during squeeze tests for Carbopol gels [22] using the rheological properties of the fluid determined independently. Here, in order to check that we effectively control the experimental procedure and its impact on the flow characteristics, we checked again the agreement between the model and the data in the preliminary squeezing phase: the theoretical prediction is very close to our experimental force vs distance curve except for the largest distance values where the lubrication theory is not expected to hold (see typical example in Figure 2).

Adhesion tests

The force vs distance curves during an adhesion test may have a different qualitative aspect. As already remarked in the pioneering study in that field [20], whatever the initial conditions these curves (see Fig.2) exhibit first a peak, followed by a progressive decrease and finally a drop towards zero corresponding to the complete separation of the material into two parts. The initial increase of the force likely corresponds to some elastic loading of the material in its solid regime associated with an inversion of the curvature of the free surface: indeed a direct inspection of the sample shows that it is almost vertical for squeeze flow and curved towards the central axis during traction (see Fig.3). It is reasonable to assume that beyond the peak most of the material is in its liquid regime. As a consequence it is natural to assume that in that case the main flow is similar to that of the squeeze flow but now in the opposite direction (towards the central axis), leading to a force amplitude again given by equation (5).

Actually there is no systematic agreement between the lubrication theory and our traction force data. An example is shown in Figure 2: there is a significant discrepancy between the theory and the experiment whereas for the preliminary squeezing phase covering the same range of distances the agreement is excellent. Moreover this discrepancy appears to significantly vary as a function of the initial aspect ratio of the sample layer. Roughly speaking the level of the traction force varies from significantly above (example in Fig.2) the theoretical curve to significantly below this curve as the initial aspect ratio increases. Our

work will provide some qualitative explanations for these observations but we shall not try to provide an accurate theory describing the force evolution in all the possible regimes. We thought preferable to start by well identifying and characterizing the different regimes rather than developing a more or less complex theory focusing on some specific cases.

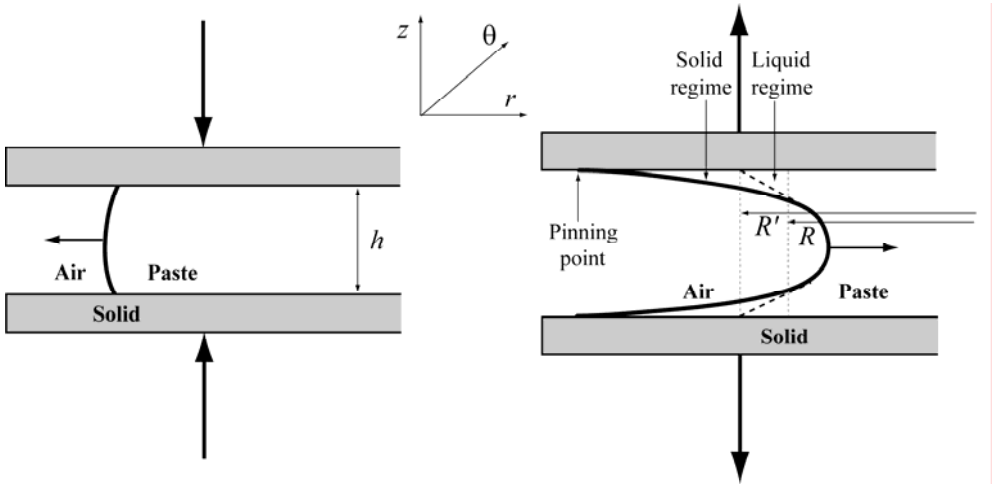

Figure 3: Aspect (in a radial cross-section) of the liquid-air interface along the periphery of the sample in the liquid regime: (left) during a squeeze test, (right) during an adhesion test. Possible distribution (see text) of the solid and liquid areas within the sample during an adhesion test.

4.2 Adhesion energy

All our data for the adhesion energy for different S_0, τ_c and Ω are presented in Figure 4. These data make it possible to determine an upper boundary of the surface tension for our material. Indeed for the largest aspect ratios the surface energy ($W_s \approx 2\gamma S_0$) computed using the value of surface tension for water is more than 3 times larger than the adhesion energy measured in our tests. So, even if viscous dissipation is negligible the theoretical surface energy computed with the above value for the surface tension is much too large to explain the experimental data. This implies that γ for our gel is less than (at least) three times smaller. Under these conditions the corresponding upper boundary of the surface energy term W_s in all our tests may be computed, and it appears to be less than 12% the adhesion energy measured for all the tests in Regime (b) and less than 25% in Regime (a) (see below). As a consequence,

in the following we will consider that the major contribution to the adhesion energy is the viscous term $W_P \approx W_v$.

Under these conditions, since at vanishing velocities in the liquid regime the stress tensor scales with the yield stress the viscous energy term ($W_v \approx W_P$) scales with the yield stress. Thus it is natural to represent the variations of the ratio of the adhesion energy per unit volume (W_P/Ω) to the yield stress, $W_P/\tau_c\Omega$, as a function of the initial aspect ratio of the sample layer, R_0/h_0 (see inset in Fig.2), or, equivalently $S_0^{1.5}/\Omega = \sqrt{\pi}R_0/h_0$. Note that in this representation the lubrication theory corresponds to a straight line since (6) may be rewritten $W_P/\tau_c\Omega = \left(4/9\sqrt{\pi}\right)S_0^{1.5}/\Omega$.

In this diagram all our data fall along a master curve, which means that we seemingly have here the general curve for the adhesion energy of yield stress fluids. However under most experimental conditions the adhesion energy is not well predicted by the lubricational theory: for small aspect ratio W_P is much larger (by a factor around 1.8) than the theoretical prediction, while for large aspect ratio it becomes much smaller and even seems to tend to a plateau. It is worth emphasizing that this result strongly contrasts with that obtained for squeeze flows for which the squeezing energy is well predicted by this theory.

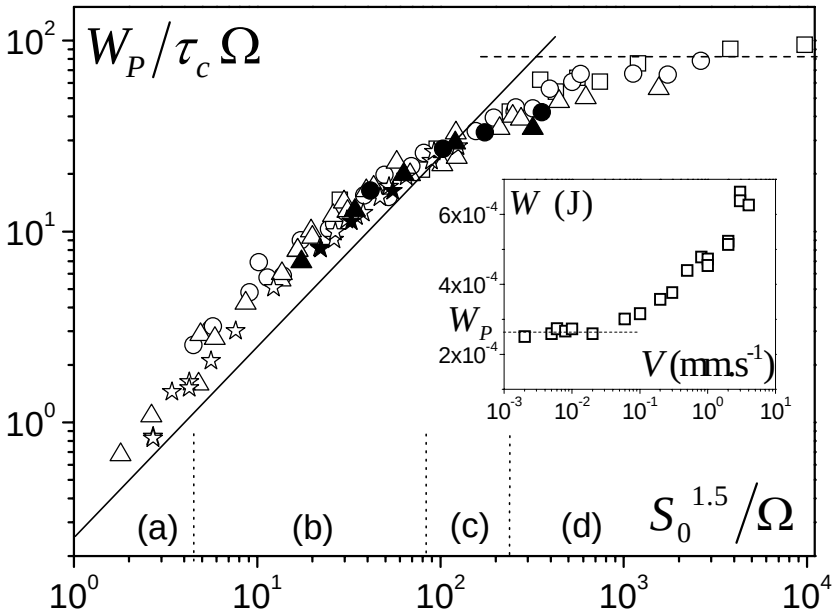

Figure 4: Dimensionless adhesion energy as a function of initial surface of contact for two different gels (open (Gel 1) and filled (Gel 2) symbols), different initial surfaces and

different sample volumes: 0.05ml (squares), 0.1ml (circles), 0.2ml (triangles), 0.5ml (stars). The continuous line is the prediction of the lubrication theory (equation (6)), the dashed lines are guides for the eye. Inset: adhesion energy for different plate separation velocities for Gel 1, with $S_0 = 5\text{cm}^2$ and $\Omega = 0.2\text{ml}$.

4.3 The different flow regimes

General observations

In order to find the origin of these discrepancies we need to have a more detailed view of the flow characteristics during an adhesion test. In that aim we focus on the aspect of the sample at the end of a test. The shape of the material layer between the plates at the end of the squeezing phase is approximately circular and of uniform thickness but different types of final shapes may be distinguished, likely associated with different flow regimes during the plate separation. Note that for each test the aspect of the deposits on the upper and lower plates are similar (one deposit is identical to the other when looked at through a mirror), which means that even if the gravity cannot always be neglected in the adhesion energy it likely does not affect the flow characteristics. Indeed the absence of gravity implies that an inertialess flow is similar when observed from a reference frame attached to either solid plate.

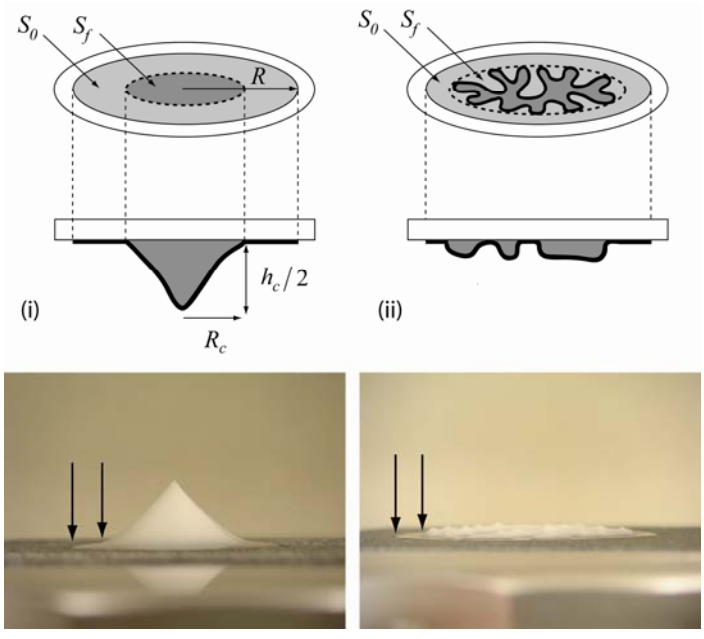

Figure 5: Main aspects of the sample deposit at the end of an adhesion test for two different flow regimes: (i) main material volume in a central region; (ii) uneven shape of the main material volume. On the upper pictures the outer extent of the initial surface of contact between the paste and the solid is represented by a light grey area while the extent

of the main material volume is represented by a dark grey area. The arrows on the photos show the limits of outer and inner boundaries of the thin layer remaining behind the main sample volume.

Characteristics of the different regimes

Typical results are as follows: at the end of the test, i.e. after complete separation of the plates, most of the material volume is either gathered around the central point and has approximately a conical shape (Fig.5 (i)), or spread over the plate in the form of a tree-like structure (Fig.5 (ii)). A critical point is that in both cases there remains a layer of material of thickness much smaller than the rest of the deposit and covering all the rest of the initial surface of contact (i.e. at the end of the squeezing phase). This means that there is a pinning effect: the line of contact (the solid-air-paste interface) remains fixed, so that during the flow the shape of the interface in a (r, z) plane has the typical aspect shown in Figure 3 (right).

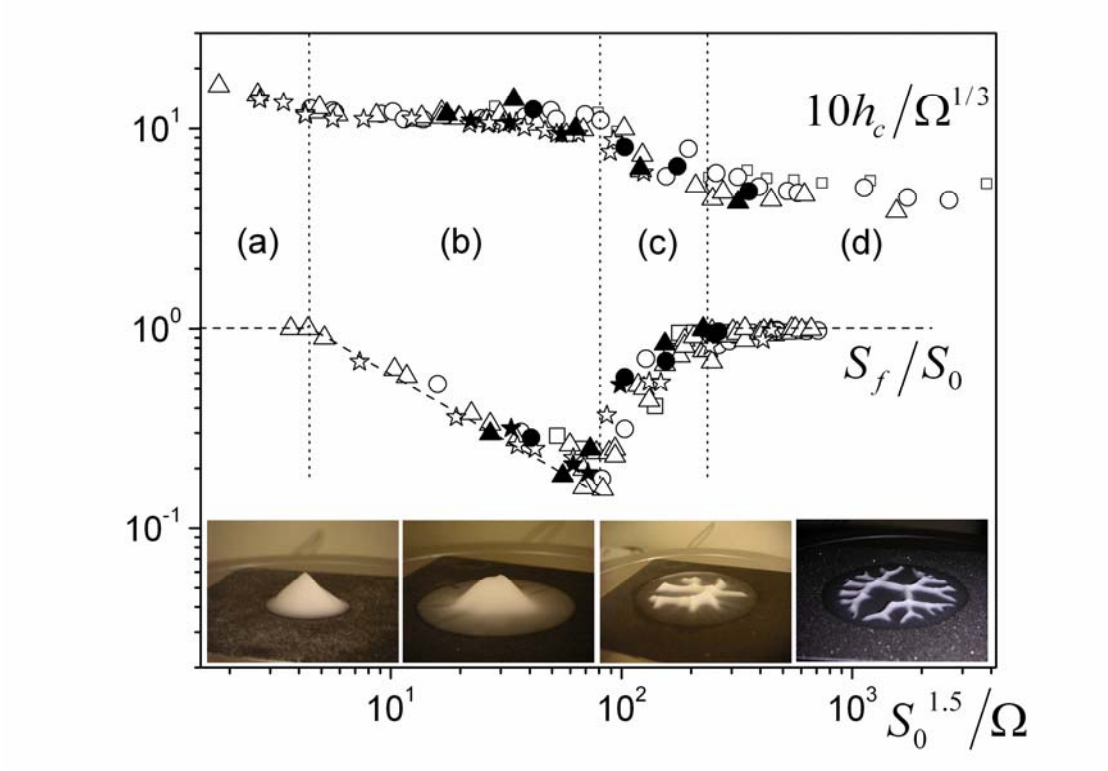

Figure 6: Geometrical characteristics of the material deposits after adhesion tests for two different gels (open symbols and filled symbols) and different sample volumes: 0.05ml (squares), 0.1ml (circles), 0.2ml (triangles), 0.5ml (stars): dimensionless critical height of separation (upper data) and (lower data) ratio of the final surface of contact to the initial one, as a function of the initial aspect ratio of the sample. The two sets of data were obtained independently. The photos (with the emulsion over a dry surface) illustrate the

different regimes (a,b,c,d) and the dashed lines correspond to our analysis of the regimes (see text).

Let us now describe more quantitatively the geometrical characteristics of the different regimes, considering different materials, initial surfaces and sample volumes. The geometrical characteristics of the final shape of the material may be mainly described with two variables: S_f/S_0, in which S_f is the area of the surface limited by the circular envelop of the main material volume (see Fig.5 (i) and (ii)); and $h_c/\Omega^{1/3}$, the dimensionless distance of separation. Four regimes, which directly correspond to the qualitative aspects of the deposits, can be clearly distinguished from the evolution (see Fig.6) of these geometrical characteristics of the sample as a function of the initial aspect ratio of the sample (R_0/h_0, or equivalently $S_0^{1.5}/\Omega$).

In the situation (i) of Figure 5 we have in fact two regimes. For very small values of R_0/h_0 (regime (a)), the final surface of contact is equal to the initial one: $S_f/S_0 = 1$. Here the radial flow is apparently limited and the vertical component of the velocity may be significant. For larger values of R_0/h_0 S_f is smaller than S_0 (regime (b)). The aspect of the final deposit (Fig. 6) suggests that there is first mainly an inward flow, as evidenced by the thin layer of fluid left behind the main volume, then a final flow of the material as in regime (a) leading to separation. The material gathers around the plate center until its geometrical characteristics reach the critical values associated with regime (a), i.e. a critical value of S_f. We expect that for a given sample volume there is a unique value of this critical value of S_f. Effectively we observe (see Fig.6) that our data is approximately aligned along $\left(S_0^{1.5}/\Omega\right)^{-2/3}$, which implies that $S_f \propto \Omega^{2/3}$. Moreover we remark that $h_c/\Omega^{1/3}$ is constant (≈ 1150) in regime (b) (see Fig.6), which suggests that for a given sample volume the separation occurs for critical geometrical conditions.

Let us further study these critical conditions. Since the sample volume may be rewritten in the form $\Omega \approx \pi R_c^2 h_c$ (R_c is the critical radius just before separation) the separation occurs at a critical value of the aspect ratio h_c/R_c. From our data ($h_c/\Omega^{1/3} \approx 1150$) we find $h_c/R_c = 2.2$. Since after separation no further flow is expected with such fluids we emphasize that this aspect ratio describes the universal shape of any deposit of yield stress fluid after separation

into two parts at vanishing velocity and in the absence of gravity effects, whatever the material volume and yield stress as long as $S_0^{1.5}/\Omega$ is in the range [4-90].

In the situation (ii) (see Fig.5) the final shape of the main material part is not circular suggesting that some instability occurs. Two different regimes can be distinguished. In regime (c) the instability seems to occur only partially during the adhesion tests since the surface envelop S_f of the corresponding tree-like structure is smaller than S_0. In contrast, in regime (d) the instability seems to start from the beginning of the adhesion test, thus leaving a tree-like structure covering the whole initial surface, and we have $S_f = S_0$ (see Fig.6). This suggests that in regime (c) the instability starts to occur but cannot develop over the whole flow and finally the fingers are somewhat moved towards the centre during a second part of the flow. Thus the critical conditions for the instability onset correspond to the transition from regime (b) to (c).

4.4 Comparison with theory

Adhesion energy in Regime (b)

In regime (b), in most cases we have $R_0 >> h_0$, so that we are in the appropriate conditions for the lubrication assumption to be valid at least at the beginning of the flow and let us remind that in that case we concluded that the expression (6) should provide an upper boundary of the effective adhesion energy. However in this regime the experimental value for W_P appears to be about twice the theoretical value associated with this theory (see Fig.4). This suggests that there is some additional effect, not taken into account in the simple lubrication theory and which provides an additional energy dissipation. It is natural to suspect that this result finds it origin in surface tension effects but we have seen (see Section 4.2) that its effect is anyway much smaller. Moreover if such an effect was to play a role it would do it in a symmetric way for adhesion and squeezing, leading to a significant discrepancy between squeeze flow data and theory, which is not the case.

Alternatively we can conjecture that, due to the pinning effect, the surface of plane in contact with flowing paste, and still flowing even slowly, is larger than that for a squeeze test at the same distance. Actually, from direct observations and from the final aspect of the deposit we are certain that the qualitative aspect of the free surface of the material at any time during the process is as shown in Figure 3. Moreover the thin layer of material remaining behind the

main volume initially flows then stops flowing. Obviously the regions the farthest from the center stop flowing first. As a consequence it is likely that at any time there is a stopped region (growing in time) along the periphery, and its boundary with the flowing region displaces radially inwards in time. Thus the effective radius of flowing material in contact with the solid plane would be R', larger than the theoretical radius R for a perfect cylindrical layer associated with the effective volume of material (see Fig.3). Then, again within the frame of the lubrication theory the pressure distribution should be related to the shear stress in a way similar to that presented in Section 3.2. The normal force, calculated from the integral of the pressure over the area of the surface of contact between the paste and the solid, would be given by (5) with now R' instead of R, finally leading to an adhesion energy larger by a factor $\left(R'/R\right)^3$. This implies that it is sufficient to have a solid-liquid limit situated at a distance larger by a factor of 20% to get a good agreement of our data with the lubrication theory in Regime (b).

This analysis simply shows that the larger adhesion energy in regime (b) may find its origin in this specific (pinning) flow effect of yield stress fluids independently of surface tension effects but a more complete analysis would require a full description of the flow characteristics.

Conversely the plateau in the adhesion energy observed in regime (d) (Fig.4) is likely due to the fact that when fingering occurs, the air fingers advance and leave behind a significant portion of the material which no longer participates in the energy dissipation.

Fingering in Regimes (c) and (d)

The irregular deformations of the initially circular liquid-air interface suggest that the Saffman-Taylor instability takes place. The different adhesion tests carried out in this study are plotted in a $\tau_c R_0^{\,2}$ vs h_0 diagram in Figure 7. The existing theory in that field predicts a transition for a set of parameters satisfying equation (7), which is represented in Figure 7 using the surface tension of water. Our analysis of Section 3.3 in fact suggests that the paste has a much smaller value, which would move the transition curve downwards. From our data (Fig.4) we find that the flow becomes unstable for $S_0^{1.5}/\Omega \approx 80$, so that the transition between stable and unstable flows occurs in our diagram (dotted line in Fig.7) at a vertical distance of

at least 3 orders of magnitude from the theoretical prediction. This suggests that the theory misses some critical aspect which has still to be identified.

Actually, reviewing the Saffman-Taylor theory for yield stress fluids [34] which simply adapted the conventional assumptions with simple fluids to these non-Newtonian materials, we remark that it is hypothesized that the curvature of the air-paste interface in a vertical plane remains constant. From our observations, due to the pinning effect, it seems strongly unlikely that this is true and this might constitute a strong stabilizing effect. Indeed let us take again the heuristic approach of Section 3.4 assuming a sinusoidal curvature of the interface (in a horizontal plane (r,θ)). This perturbation still induces an additional viscous pressure drop term $(\approx 2\tau_c\varepsilon/h)$ and a surface tension pressure drop term due to the curvature in the horizontal plane $(\approx 4\pi^2\gamma\varepsilon/\lambda^2)$. However the pinning and this perturbation also likely induce a change in the curvature of the interface in a vertical plane (r,z) (see Figure 3), which induces an additional surface tension pressure drop. For example, if the shape of the interface in the plane (r,z) is an ellipse of height h along z and depth d along x the additional pressure drop due to an increase of d to $d+\varepsilon$, is $4\gamma\varepsilon/h^2$. This term is generally much larger than the term due to the curvature in the horizontal plane (except if $\lambda \approx h$), which suggests that the theoretical predictions should be significantly different by taking this term into account.

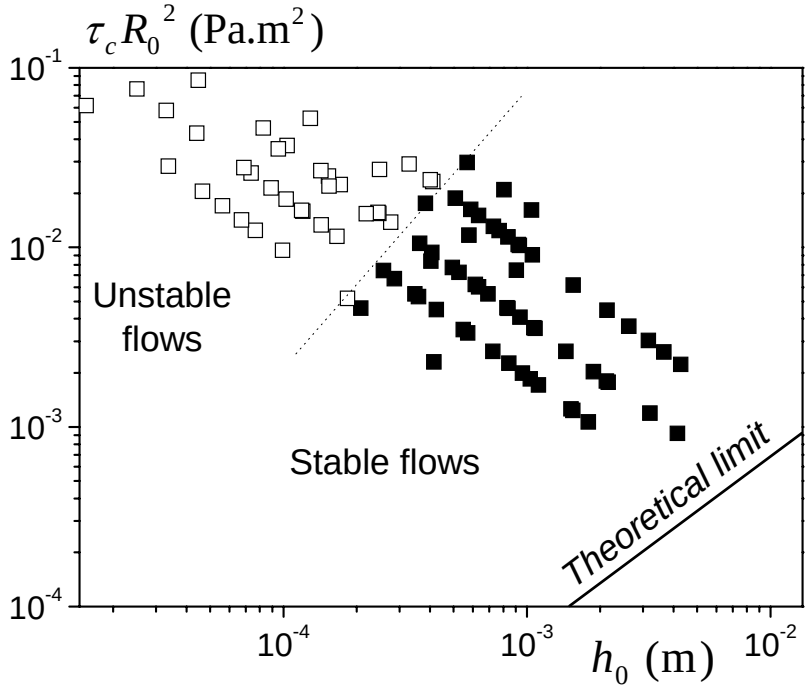

Figure 7: Distribution of the stable (filled squares) and unstable (empty squares) flows during our adhesion tests in a $\tau_c R_0^2$ vs h_0 diagram (tests presented in Figure 6). The continuous line is the theoretical limit between the two regimes according to equation (7) with the surface tension of water. The dotted line corresponds to transition criterion identified experimentally, i.e. $S_0^{1.5}/\Omega = 80$.

At this stage this simply means that the pinning effect, by fixing the line of contact, tends to induce larger surface tension effects stabilizing the flow, but a more complete theory taking into account all the characteristics of the flow and the shape of the interface has still to be developed.

5. Conclusion

These results show that the adhesion of pastes, and in particular simple yield stress fluids, have original specificities. Different regimes have been identified which are supposed to describe the whole range of possible trends with such materials. In particular we have shown that in a specific range of initial aspect ratios the final sample shape is conical with a given aspect ratio whatever its volume. Moreover we have shown that in this regime the adhesion energy is significantly larger than the theoretical energy associated with a simple lubricational flow. This contrasts with the opposite flows, i.e. squeeze flows, for which there is a good agreement between theory and experiments. We attributed this effect to the pinning effect observed with these materials: the line of contact remains fixed so that the material flows in a slightly larger region along the solid plates than assumed from the theory with the same effective volume. The detailed characteristics of such a flow need to be studied in more details either analytically or by numerical simulations.

Another striking result of our work is the fact that the occurrence of viscous fingering is not at all predicted by the conventional Saffman-Taylor theory for yield stress fluids. This theory is nothing more than the extrapolation of the theory for simple fluids taking into account the specificity of pastes. Thus, if the main physical phenomena were correctly identified this theory should predict at least roughly the experimental conditions of development of the instability. The strong discrepancy observed suggests that we are missing a significant effect in this Saffman-Taylor theory for yield stress fluids and more generally in the adhesion of pastes in this regime.

More generally our work also emphasized the current poor knowledge in the field of interfacial problems with pasty materials. For example there is still a wide uncertainty on the value of surface tension which should be taken into account in the models, and there is no obvious technique for measuring it. Another example is the impact of wall slip of pastes along smooth surfaces, a question that we were able to avoid by using appropriate rough surfaces but which might play a significant role in adhesion with smooth solid surfaces. More insight in those fields should be gained from new experiments involving different flow types such as the spreading of a paste droplet [], maybe at very different scales and with various surface types, and from an analytical or numerical description of the local flow characteristics.

Acknowledgements: This work was made possible through the financial support of ANR, within the frame of the project PHYSEPAT ANR-05-BLAN-0131.

References

[1] A.J. Liu, and S.R. Nagel, *Nature*, 1998, 396, 21

[2] J. Vermant and M.J. Solomon, *J. Phys. Cond. Matter.*, 2005, 17, 18

[3] P. Coussot, *Soft Matter*, 2007, 3, 528

[4] J. Goyon, A. Colin, G. Ovarlez, A. Ajdari, L. Bocquet, *Nature*, 2008, 454, 84

[5] J. Mewis and N.J. Wagner, *J. Non-Newt. Fluid Mech.*, 2009, 157, 147

[6] S.M. Fielding, M.E. Cates and P. Sollich, *Soft Matter*, 2009, DOI: 10.1039/b812394m

[7] J. Israelachvili, *Intermolecular and Surface Forces*, Academic Press (1985-2004)

[8] L. Bécu, S. Manneville, and A. Colin, *Phys. Rev. Lett.*, 2006, 96, 138302

[9] A. Ragouilliaux et al., *Phys. Rev. E*, 2007, 76, 051408

[10] P. Coussot et al., *J. Non-Newt. Fluid Mech.*, 2009, 158, 85

[11] J.J. Bikerman, *J. Colloid Sci.*, 1947, 2, 163

[12] C. Gay, and L. Leibler, *Phys. Today*, 1999, 52, 48

[13] K.R. Shull, C.M. Flanigan, and A. Crosby, *Phys. Rev. Lett.*, 2000, 84, 3057

[14] J.A.F. Harvey and D. Cebon, *J. Mater. Sci.*, 2003, 38, 1021

[15] A. Lindner, D. Derks, M.J. Shelley, *Phys. Fluids*, 2005, 17, 072107

[16] S. Sinha, T. Dutta, and S. Tarafdar, *Eur. Phys. J. E*, 2008, 25, 267

[17] J. Nase, A. Lindner, C. Creton, *Phys. Rev. Lett.*, 2008, 101, 074503

[18] H. Lemaire et al., *Fractals*, 1993, 1, 968

[19] Y.O.M. Abdelhaye, M. Chaouche, H. Van Damme, *Appl. Clay Sci.*, 2008, 42, 163

[20] D. Derks et al., *J. Appl. Phys.*, 2003, 93, 1157

[21] J.M. Piau, *J. Non-Newt. Fluid Mech.*, 2007, 144, 1

[22] B. Rabideau, C. Lanos, P. Coussot, *Rheol. Acta*, 2009, 48, 517

[23] G. Ovarlez et al., *Phys. Rev. E*, 2008, 78, 036307

[24] V. Bertola et al, *J. Rheol.*, 200347, 1211

[25] P. Coussot, *Rheometry of pastes, suspensions and granular materials* (Wiley, New York, 2005)

[26] G.H. Meeten, *Rheol. Acta*, 2002, 41, 557

[27] J. Engmann, C. Servais, A.S. Burbridge, *J. Non-Newt. Fluid Mech.*, 2005, 132, 1

[28] G.H. Covey, and B.R. Stanmore, *J. Non-Newt. Fluid Mech.*, 1981, 8, 249

[29] R. Blanc, H. Van Damme, Ch.9, in *Mobile particulate systems*, E. Guazzelli, L. Oger (eds.) (Kluwer, Amsterdam, 1995)

[30] Y. Yoshitake et al., *Phys. Rev. E*, 2008, 78, 041405

[31] S. Tarafdar and S. Roy, *Fractals*, 1995, 1, 99

[32] P.G. Saffman and G. Taylor, *Proc. R. Soc. Lond.*, 1958, A245, 312

[33] G.M. Homsy, *Ann. Rev. Fluid Mech.*, 1999, 19, 271

[34] P. Coussot, *J. Fluid Mech.*, 1999, 380, 363

[35] S.D.R. Wilson, *J. Fluid Mech.*, 1990, 220, 413

[36] J.E. Sader, D.Y.C. Chan, and B.D. Hughes, *Phys. Rev. E*, 1994, 49, 420

[37] L. Kondic, P. Palffy-Muhoray, and M.J. Shelley, *Phys. Rev. E*, 1996, 54, R4536

[38] A. Lindner, D. Bonn, and P. Coussot, *Physical Review Letters*, 2000, 85, 314

[39] L.H. Luu, and Y. Forterre, J. Fluid Mech., 2009, 632, 301